J|A|C|S COMMUNICATIONS

Published on Web 05/19/2010

Highly-Selective and Reversible O_2 Binding in Cr_3(1,3,5-benzenetricarboxylate)$_2$

Leslie J. Murray,[†] Mircea Dinca,[†] Junko Yano,[‡] Sachin Chavan,[§] Silvia Bordiga,[§] Craig M. Brown,[||] and Jeffrey R. Long*,[†]

Department of Chemistry, University of California, Berkeley, California 94720, Physical Biosciences Division, Lawrence Berkeley National Laboratory, Berkeley, California 94720, Department of Chemistry, IFM & NIS Centre of Excellence, University of Torino, Via Quarello 11 I-10135 Torino, Italy, and Center for Neutron Research, National Institute of Standards and Technology, Gaithersburg, Maryland 20899

Received April 2, 2010; E-mail: jrlong@berkeley.edu

The separation of O_2 from air is carried out in industry using cryogenic distillation on a scale of 100 Mtons/year,[1] as well as using zeolites in portable devices for medical applications.[2] Thus, there is a clear benefit to developing materials that might enable this process to be carried out with a lower energy cost. Recently, the need for such materials has become even more apparent, owing to the potential for using oxyfuel combustion as a means of eliminating CO_2 emissions from fossil fuel-fired power plants.[3] Here, instead of separating CO_2 from N_2, as in postcombustion capture, O_2 is separated from the N_2 in air prior to combustion. Advantages of this scenario include the greater partial pressure of O_2 in air (0.21 bar) compared to CO_2 in a typical flue gas (0.10−0.15 bar) and the fact that, although pure O_2 is needed, it is not necessary to remove 100% of it from the air stream.

In addition, there is the chemical advantage of being able to distinguish O_2 from N_2 via its greater propensity for accepting negative charge transferred from a redox-active transition metal center. Indeed, this mechanism provided the foundation for a great deal of chemistry involving molecular complexes, particularly of cobalt(II), used for the reversible capture and transport of O_2.[4] By isolating such transition metal centers within the pores of a zeolite,[5] it is further possible to inhibit the formation of O_2-bridged structures that can diminish the performance of molecular complexes. For example, Cr^{2+} ions exchanged into zeolite A led to a reversible O_2 loading of 2.7 wt % at 298 K.[5a] We envision that metal−organic frameworks, which can present both high surface areas and open metal coordination sites,[6] may form the basis for a new generation of O_2 capture materials with good air permeability, a high loading capacity, and a tunable O_2 adsorption enthalpy. Herein, we report the synthesis of the first Cr^{II}-based metal−organic framework, $Cr_3(BTC)_2$ (BTC^{3-} = 1,3,5-benzenetri-carboxylate), which displays both a high O_2 loading capacity and strong selectivity for binding O_2 over N_2 at 298 K.

Analogous to the synthesis of $Mo_3(BTC)_2$,[7] the reaction of $Cr(CO)_6$ with trimesic acid in DMF yielded $Cr_3(BTC)_2 \cdot n$DMF as a purple microcrystalline solid. X-ray powder diffraction data revealed the compound to be isostructural with $Cu_3(BTC)_2 \cdot 3H_2O$.[8] It thus features the porous three-dimensional framework structure depicted in Figure 1A, wherein $Cr_2(O_2CR)_4(DMF)_2$ paddle-wheel complexes are linked via triangular BTC^{3-} bridging ligands. The DMF solvent was exchanged with methanol, and the material was desolvated by heating at 160 °C under vacuum for 48 h to afford $Cr_3(BTC)_2$ as a yellow-green solid. Once activated, the compound reacts rapidly in air to generate a deep forest green solid.

Rietveld analysis of powder neutron diffraction data collected for $Cr_3(BTC)_2$ showed retention of the framework structure, albeit with a shortening of the intermetal separation within the paddle-wheel units.

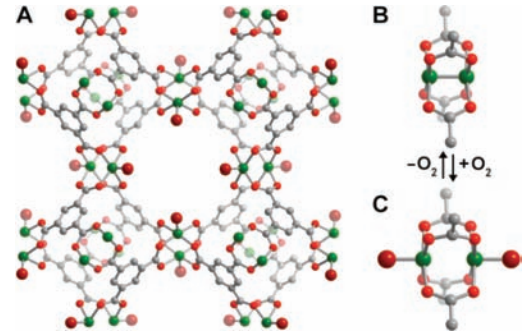

Figure 1. Portions of the structure of $Cr_3(BTC)_2$, where green, red, and gray spheres represent Cr, O, and C atoms, respectively, while large red spheres represent either bound DMF molecules in the solvated structure or bound O_2 molecules upon desolvation and exposure to O_2. Atomic positions shown correspond to the results obtained from Rietveld refinement of powder neutron diffraction data for activated (B) and O_2-loaded (A and C) samples. Note that the Cr−Cr distance lengthens from 2.06(2) Å in B to 2.8(1) Å in C upon coordination of O_2.

The observed distance of 2.06(2) Å is in line with the formation of a Cr−Cr quadruple bond upon loss of the axial solvent molecules.[9] Consistent with this open framework structure, the N_2 gas adsorption isotherm measured at 77 K revealed a type I adsorption isotherm with BET and Langmuir surface areas of 1810 and 2040 m^2/g, respectively (Figure S1). The latter value is comparable to the Langmuir surface areas of 2175 and 2010 m^2/g determined for $Cu_3(BTC)_2$[10] and $Mo_3(BTC)_2$,[7] respectively.

Given the likelihood that the exposed Cr^{II} centers might engage in charge transfer interactions with O_2 but not N_2, $Cr_3(BTC)_2$ was tested for the selective uptake of O_2 at 298 K (Figure 2). Indeed, while the N_2 adsorption isotherm climbs gradually to a capacity of 0.58 wt % at 1 bar, the O_2 isotherm rises sharply, reaching 11 wt % at just 2 mbar. The latter loading corresponds to ∼0.8 molecules of O_2 per Cr center, near the value of 1 (or 14.4 wt %) expected if every metal in the framework were available to bind an O_2 molecule. Based on interpolated uptakes of 0.73 mmol/g O_2 at 0.21 bar and 0.033 mmol/g N_2 at 0.78 bar (reflecting the corresponding partial pressures in air), $Cr_3(BTC)_2$ exhibits an exceptional O_2/N_2 selectivity factor of 22. To our knowledge, the highest selectivity factor observed previously is ∼4 for cobalt(II) complexes appended to a silica support.[11] Moreover, both the selectivity and gravimetric capacity are much greater than previously reported for O_2 uptake in any metal−organic framework.[12]

The temperature and evacuation time required to release O_2 to regenerate the capture material were tested. Heating at 50 °C under dynamic vacuum for 48 h was optimal and afforded a material that readsorbed O_2 with a somewhat reduced capacity of 9.1 wt % at 0.21 bar. As shown in the inset of Figure 2, repeated cycling performed on a separate sample under such conditions indicated a gradual reduction

[†] University of California.
[‡] Lawrence Berkeley National Laboratory.
[§] University of Torino.
[||] National Institute of Standards and Technology.

10.1021/ja1027925

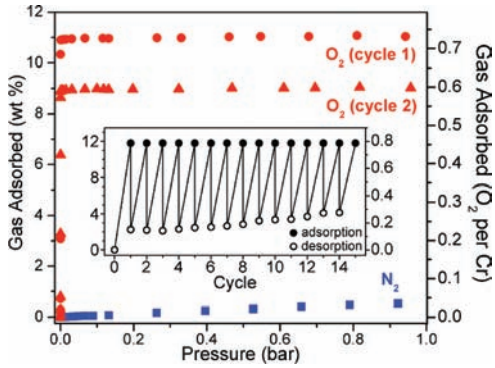

Figure 2. Uptake of O_2 (red symbols) and N_2 (blue squares) by $Cr_3(BTC)_2$ at 298 K. The compound saturates with O_2 at ~2 mbar but shows little affinity for N_2. Upon evacuation, the O_2 isotherm for a second cycle reveals a slightly reduced capacity, while the isotherm for a third cycle (not shown) is essentially identical to the second. Inset: Uptake and release of O_2 by a different sample of $Cr_3(BTC)_2$ over 15 consecutive cycles at 298 K. Desorption was carried out by heating at 50 °C under vacuum for 48 h.

in the O_2 loading capacity. This behavior is likely a consequence of incomplete release of bound O_2 under the regeneration conditions and/or partial decomposition of the material as a result of the highly exothermic reaction with O_2. Consistently, we observed a 5% loss in surface area of the material after the two cycles (Figure S1), only minor changes to the powder X-ray diffraction patterns upon oxygenation (Figure S3), and an increase in sample weight after the first O_2 desorption cycle.

The nature of the interaction between $Cr_3(BTC)_2$ and O_2 was probed using a variety of spectroscopic techniques. As shown at the right in Figure 3, upon exposure to O_2 an infrared absorption band at 1129 cm^{-1} appears and increases in intensity with dosage (Figures 3, S6). We assign this band to a ν_{O-O} vibrational mode and note that its frequency lies between those previously assigned for a Cr^{III}-η^2-superoxide species (1027−1104 cm^{-1})[13] and a putative end-on superoxide moiety bound to a Cr^{III} porphyrin complex (1142 cm^{-1}).[14] Two additional, weaker absorption features are also observed, and we attribute these to an overtone of the 1129 cm^{-1} mode and to a ν_{O-O} mode arising from a superoxide or peroxide adduct (see Supporting Information). In the UV−vis−nIR spectra, new absorption features at 13 430, 15 840, and 20 600 cm^{-1} are observed upon exposure to O_2 (Figure 3, left). These bands disappear after deoxygenation of the sample, consistent with the reversible O_2 binding observed in the gas uptake experiments.

In an effort to determine the oxidation state of chromium in the O_2-loaded sample, X-ray absorption spectra of the DMF-solvated, activated, and oxygenated frameworks were measured (Figure S7). Two intense absorption maxima at 5996 and 5992 eV, consistent with a square pyramidal Cr coordination geometry, are evident in the spectrum of the activated sample. These transitions are expectedly weaker in the solvated and O_2-loaded samples, indicating coordination at the axial sites of the paddle-wheel units. Significantly, the first moment energy increases by 0.07 eV in going from the activated to the oxygenated samples (Figure S8). This, together with the infrared spectrum, suggests that there is partial charge transfer from the Cr^{II} center to the bound O_2 molecule but not necessarily complete charge transfer to give a Cr^{III}-superoxide adduct.

A Rietveld refinement of neutron powder diffraction data collected at 4 K on a sample of $Cr_3(BTC)_2$ loaded with ~1 equiv of O_2 per Cr atom provides direct structural evidence for the binding of O_2 to the metal centers. The best fit afforded a model in which 0.87(3) O_2 molecules are coordinated to the axial sites of each paddle-wheel unit (Figure 1), while 0.197(7) occupy the smallest pore openings within the framework (Figure S5). The model further indicates an increased Cr−Cr separation of 2.8(1) Å and a distance of 1.97(5) Å between

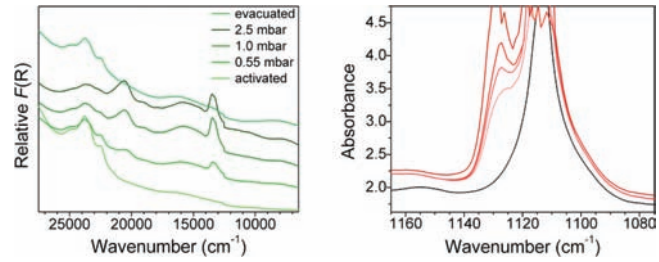

Figure 3. Diffuse reflectance UV−vis−nIR (left) and infrared (right) spectra of $Cr_3(BTC)_2$ under various loadings of O_2. On the right, dosage of O_2 increases from the black (no O_2) to pink to dark red traces.

the Cr atom and the centroid of the bound O_2 molecule (Table S3). We note that although the resolution of the data was insufficient to determine the orientation of O_2, the observed metal−centroid distance is more likely consistent with a side-on coordination mode.

The foregoing results demonstrate the reversible, selective binding of O_2 at a high loading capacity within $Cr_3(BTC)_2$, a metal−organic framework featuring open Cr^{II} coordination sites. Future work will attempt to improve framework stability and reduce the energy required for deoxygenation by varying the metal or attenuating the donor strength of the bridging ligand through addition of electron-donating/withdrawing substituents.

Acknowledgment. This research was supported by the Department of Energy under Awards FG36-05GO15002 (early stages) and DE-SC0001015 (later stages). We thank J.-H. Her and Dr. W. Weare for experimental assistance.

Supporting Information Available: Full experimental details. This material is available free of charge via the Internet at http://pubs.acs.org.

References

(1) Greenwood, N. N.; Earnshaw, A. *Chemistry of the Elements*, 2nd ed.; Butterworth Heinemann: Burlington, MA, 2002; p 604.
(2) Nandi, S. P.; Walker, P. L., Jr. *Sep. Sci. Technol.* **1976**, *11*, 441.
(3) (a) Buhre, B. J. P.; Elliott, L. K.; Sheng, C. D.; Gupta, R. P.; Wall, T. F. *Prog. Energy Combust. Sci.* **2005**, *31*, 283. (b) Kanniche, M.; Gros-Bonnivard, R.; Jaud, P.; Valle-Marcos, J.; Amann, J.-M.; Bouallou, C. *Appl. Therm. Eng.* **2009**, *30*, 53.
(4) (a) Calvin, M.; Bailes, R. H.; Wilmarth, W. K. *J. Am. Chem. Soc.* **1946**, *68*, 2254. (b) Ramprasad, D.; Pez, G. P.; Toby, B. H.; Markley, T. J.; Pearlstein, R. M. *J. Am. Chem. Soc.* **1995**, *117*, 10694. (c) Ramprasad, D.; Markley, T. J.; Pez, G. P. *J. Mol. Catal. A: Chem.* **1997**, *117*, 273. (d) Corriu, R. J. P.; Lancelle-Beltran, E.; Mehdi, A.; Reye, C.; Brandès, S.; Guilard, R. *J. Mater. Chem.* **2002**, *12*, 1355.
(5) (a) Kellerman, R.; Hutta, P. J.; Klier, K. *J. Am. Chem. Soc.* **1974**, *96*, 5946. (b) Jayaraman, A.; Yang, R. T.; Cho, S. H.; Bhat, T. S. G.; Choudary, V. N. *Adsorption* **2002**, *8*, 271. (c) Mishra, D. In *Recent Advances in the Science and Technology of Zeolites and Related Materials, Parts A-C*; VanSteen, E., Claeys, M., Callanan, L. H., Eds.; 2004; Vol. 154, p 1693.
(6) (a) Eddaoudi, M.; Kim, J.; Rosi, N.; Vodak, D.; Wachter, J.; O'Keeffe, M.; Yaghi, O. M. *Science* **2002**, *295*, 469. (b) Kitagawa, S.; Kitaura, R.; Noro, S.-I. *Angew. Chem., Int. Ed.* **2004**, *43*, 2334. (c) Férey, G. *Chem. Soc. Rev.* **2008**, *37*, 191. (d) Dinca, M.; Long, J. R. *Angew. Chem., Int. Ed.* **2008**, *47*, 6766, and references therein.
(7) Kramer, M.; Schwarz, U.; Kaskel, S. *J. Mater. Chem.* **2006**, *16*, 2245.
(8) Chui, S. S. Y.; Lo, S. M. F.; Charmant, J. P.-H.; Orpen, A. G.; Williams, I. D. *Science* **1999**, *283*, 1148.
(9) (a) Cotton, F. A.; Rice, G. W. *Inorg. Chem.* **1978**, *17*, 2004. (b) Ketkar, S. N.; Fink, M. *J. Am. Chem. Soc.* **1985**, *107*, 338. (c) Cotton, F. A.; Hillard, E. A.; Murillo, C. A.; Zhou, H.-C. *J. Am. Chem. Soc.* **2000**, *122*, 416.
(10) Wong-Foy, A. G.; Matzger, A. J.; Yaghi, O. M. *J. Am. Chem. Soc.* **2006**, *128*, 3494.
(11) Dubois, G.; Tripier, R.; Brandès, S.; Denat, F.; Guilard, R. *J. Mater. Chem.* **2002**, *12*, 2255.
(12) (a) Li, Y.; Yang, R. T. *Langmuir* **2007**, *23*, 12937. (b) Maji, T. K.; Matsuda, R.; Kitagawa, S. *Nat. Mater.* **2007**, *6*, 142. (c) Mu, B.; Schoenecker, P. M.; Walton, K. S. *J. Phys. Chem. C* **2010**, *114*, 6464. (d) Xue, M.; Zhang, Z.; Xiang, S.; Jin, Z.; Liang, C.; Zhu, G.-S.; Qiu, S.-L.; Chen, B. *J. Mater. Chem.* **2010**, *20*, 3984.
(13) Qin, K.; Incarvito, C. D.; Rheingold, A. L.; Theopold, K. H. *Angew. Chem., Int. Ed.* **2002**, *41*, 2333.
(14) Cheung, S. K.; Grimes, C. J.; Wong, J.; Reed, C. A. *J. Am. Chem. Soc.* **1976**, *98*, 5028.

JA1027925